Appl Nanosci (2014) 4:551–569
DOI 10.1007/s13204-013-0230-0

ORIGINAL ARTICLE

Effects of pyrolysis conditions on the porous structure construction of mesoporous charred carbon from used cigarette filters

Salman Masoudi Soltani · Sara Kazemi Yazdi · Soraya Hosseini

Received: 4 April 2013 / Accepted: 3 May 2013 / Published online: 15 May 2013

Abstract One-step pyrolysis was applied to synthesize mesoporous charred carbon from used cigarette filters. Proximate analysis suggested that cigarette filters are decent carbon precursors due to their moderate carbon (around 11 %) and low ash (around 0.1 %) contents. To investigate the effects of pyrolysis parameters on porous surface area, a full factorial design of experiment including heating rate, soaking time and pyrolysis temperature was used with each factor at three levels. The analysis of variance revealed that the temperature and heating rate had the most significant effects on total surface area of the synthesized carbon. Response surface model (RSM) was applied to best fit a surface through the experimental data. It was seen that the quadratic RSM model with a reasonable R^2 value of 63 % was the best developed model. The maximum BET surface area (597 m^2/g) was reached at a pyrolysis temperature of 900 °C when the precursor was heated at 5 °C/min and hold at this temperature for 3 h. The produced N_2 adsorption–desorption isotherm showed a certain degree of mesoporosity in the charred carbon with an average pore size of 3.32 nm calculated by Barrett–Joyner–Halenda method. Scanning electron microscopy also showed the presence of macroporosity on the charred carbon surface. Fourier transform infrared spectroscopy revealed the presence of acidic surface functional groups such as carboxyl and phenol which were accordingly confirmed by Boehm titration. In addition, Boehm titration showed that the produced carbon's surface was more acidic than basic in nature.

Keywords Pyrolysis · Mesoporous charred carbon · Response surface method

S. Masoudi Soltani (✉) · S. K. Yazdi
Department of Chemical and Environmental Engineering, The University of Nottingham, Broga Rd, 43500 Semenyih, Selangor, Malaysia
e-mail: smasoudis@gmail.com

S. Hosseini
Department of Chemical and Environmental Engineering, Universiti Putra Malaysia, 43400 Serdang, Selangor, Malaysia

Introduction

In search of low-cost adsorbents

There have been numerous research works done to produce and investigate low-cost adsorbents. These studies have been specifically focused on the use of waste materials and their ability to remove certain substances including organic and inorganic from waste streams (Dias et al. 2007). Although these materials have proven to be efficient to some extent, however, active carbons have shown a much better capability to remove such compounds. Nevertheless, active carbon production is currently quite costly. The production cost can be moderated either by choosing a cheap carbonaceous raw material or by applying an economical synthesis technique (Lafi 2001). There still exists the need to produce active carbon from low-cost substances synthesized at lower temperatures (less energy cost) (Sudaryanto et al. 2006). Using waste materials to produce active carbon is currently very attractive on the grounds that not only this leads to a decrease in the disposal costs on waste materials but it can consequently help to preserve the environment (Dias et al. 2007). In "Pyrolysis procedure", a brief introduction to the works done so far to convert waste materials to active carbon has been presented. These included conventional (agricultural and wood base) and non-conventional wastes.

Among non-conventional wastes, plastic wastes, different industrial wastes such as fly ash, pitch as well as polymeric residues, tires and sewage sludge have been studied and used to produce active carbons. Carbons produced from these wastes have found their ways in the adsorption of a broad range of substances including phenol and its derivatives, various kinds of dyes and also heavy metals such as nickel, mercury and copper (Dias et al. 2007).

Cigarette butts and their environmental concerns

Disposed cigarette butts are one of the biggest solid wastes produced worldwide each year. They are known to be the most-collected waste item on the beach (Smith and Novotny 2011). They pose significant environmental contamination. They are known to be toxic and hazardous waste (Barnes 2011). Environmental hazards may be resulted from the leaching of toxic components from the disposed cigarette butt filters and smoked tobacco. These include Al, Br, Cd, Cr, Cu, Fe, Pb, Mn, Ni, Sr, Ti and Zn (Moerman and Potts 2011). Moreover, these leachates when released into the aquatic environment may cause exposure not only to heavy metals but also ethyl phenol and pesticide residues (Novotny et al. 2011). This contamination by cigarette butts thrown out of the windows of moving cars, dropped on sidewalks and left on the beach is serious when they eventually find their ways to the street drains and then to the streams, rivers and oceans (Novotny et al. 2009).

The butts themselves are a threat to human infants and animals' health due to indiscriminate eating behavior (Novotny et al. 2011). With around 766,571 metric tons of cigarette butts being manufactured each year (Smith and Novotny 2011), a significant challenge has to be tackled to devise appropriate disposal regulations. These mainly owe to the existence of millions disposal points which necessitate the need to segregate collect and dispose of butts in a properly safe manner (Barnes 2011). Albeit various disposal strategies have been proposed and practiced, however, none has been effective enough so far. These alternatives include producing biodegradable filter and distributing permanent and portable ashtrays. Interestingly enough, smokers were seen to opt for discarding cigarettes butts even more knowing that the filters are biodegradable (Smith and Novotny 2011).

Cigarette butts as a potential carbon source

Nearly all cigarette filters produced in the United States of America are made up of cellulose acetate which is a plastic product. Each filter consists of around 12,000 cellulose acetate fibers (Novotny et al. 2009). These fibers contain delustrant titanium dioxide. A plasticizer, triacetin (glycerol triacetate) is also added to the fiber as a fiber binder (Longwood Education 2011). Cellulose acetate is one of the most important cellulose derivatives (Rodrigues Filho et al. 2008). It has a molecular formula of $C_{76}H_{114}O_{49}$ with an average molecular weight of 1,811.68896 g/mol (PubChem Compound 2011). It contains a high degree of carbon atoms and can potentially be nominated as an initial carbonaceous raw material for the production of porous carbon. Cellulose containing materials have been already reported to be decent precursors for carbonization (Polarz et al. 2002). Carbonization of cigarette butts has been barely reported in the literature. Polarz et al. (2002) studied the carbonization of cigarette filters in a limited carbonization conditions. They produced charred carbon by carbonizing cigarette filters at 1,000 °C for a prolonged period of 7 h with a very slow heating rate of 1 °C/min. The resulted carbon was reported to have a BET surface area of only 262 m^2/g with a porosity of 0.21 cm^3/g. Moreover, they provided that their synthesized carbon contained pores in both mesoporous and macroporous regions. However, the BET surface area was small enough to find a practical application. The carbonization parameters can be further studied and tuned to reach a higher BET surface area.

Effects of carbonization parameters on final porous carbon

Not too many research works have been done so far to investigate the effects of carbonization parameters on final porous structure of produced porous carbon. The studied parameters were mainly limited to carbonization temperature, heating rate and soaking time (reaction time). There seems to be a growing interest in the very recent years in understanding the effects of carbonization parameters on final BET surface area of final produced carbon.

Lua et al. (2004) studied the effects of pyrolysis temperature, reaction time, heating rate and nitrogen gas flow rate on the properties of char produced through the carbonization of pistachio nut shells. The optimum carbonization conditions were found to be at a temperature of 500 °C, 2 h of reaction time, a heating rate of 10 °C/min and a gas flow of 150 cm^3/min. The final carbon showed a maximum BET area of 778 m^2/g. They studied a broad range of temperatures from 250 to 1,000 °C. The reaction time varied between 1 and 3 h while the studied heating rate ranged between 5 and 40 °C/min. Their study, however, did not lead to the derivation of any model. Moreover, their strategy to study the carbonization effects was to apply the one-factor-at-a-time rather than changing all factors simultaneously. This approach is a deadly alternative technique in statistical analyses since the interactions between various factors can be simply ignored while a factorial analysis of the effects is the only way to detect

any possibly hidden interactions. The drawback of the applied method is the inefficiency in accuracy level of the produced results while often requiring more experiments (Montgomery and Runger 2011). Nevertheless, they concluded that carbonization temperature was the most influential factor on the final carbon porous structure. Barbooti et al. (2004) also investigated the effects of pyrolysis temperature (400–460 °C) and nitrogen gas flow rate (0.2–0.5 m^3/h) on the carbon yield produced by carbonization of scrap tires. Lua et al. (2006) reported a similar research on the influence of pyrolysis conditions on pore development of oil-palm shells' activated carbons. Their previous analytical method of one-factor-at-a-time was similarly applied. The optimum conditions were reported to be achieved at a temperature of 600 °C, a reaction time of 2 h and a heating rate of 10 °C/min with a nitrogen gas flow rate of 150 cm^3/min. The final activated carbon had a BET surface area of 519 m^2/g.

Haykiri-Acma et al. (2006) studied the pyrolysis yield of rapeseed. The experiments were run up to a temperature of 1,273 K at varying heating rates of 5, 10, 20, 30, 40 and 50 °C/min with a constant nitrogen gas flow of 40 m^3/min. In another reported study by Jia and Lua (2008), oil-palm shells were carbonized to produce activated carbon. They investigated the effects of temperature and reaction time on the physical characteristics of final porous carbon. The optimum pyrolysis conditions were understood to be at a temperature of 675 °C and a reaction time of 2 h. The effects of pyrolysis temperature and heating rate were also studied by carbonizing rice straw with a constant reaction time of 1 h under nitrogen gas flow (Fu et al. 2012). They concluded that temperature had the most significant effect on final porous structure of charred carbon. Carbonization of Algerian date pits was similarly studied by Bouchelta et al. (2012). The studied parameters included temperature, heating rate, reaction time and nitrogen gas flow rate. The optimum conditions were reported to be achieved at a temperature of 700 °C, a heating rate of 10 °C/min and a reaction time of 1 h. Their approach to study the carbonization effects was also confined to the one-factor-at-a-time technique. Pistachio nut-shells pyrolysis was later investigated again (Acikalin et al. 2012). In their study, pyrolysis temperature (350–650 °C), reaction time (10–50 min) and nitrogen gas flow rate (50–450 ml/min) were studied. Identical to the previous studies, they concluded that carbonization temperature had the most significant effect on the product yield.

All these and other similar works have either studied a limited range of conditions designed in a one-factor-at-a-time statistical framework or the study has been focused only on one factor while other factors have been fixed at prescribed values. Although, there have been few reports on applying a full factorial design of experiment to study the effect of synthetic conditions on final properties of the produced carbon, there exist no such research approach on the pyrolysis conditions. Barbooti et al. (2004) designed a fractional factorial experiment with temperature (400–460 °C), gas flow rate (0.2–0.5 m^3/h) and precursor particle size (2–20 mm) to investigate the effects of these parameters on the final carbonization yield of carbon black produced from scrap tires. Their study resulted in the development of a non-linear second-order response surface. In another study (Alkhatib et al. 2011), similarly, one-step pyrolysis was used to produce activated carbon from oil palm empty fruit bunch fibers under various levels of parameters including temperature (600–900 °C), steam flow rate (2–4 ml/min) and activation time 15–45 min). In their study they took advantage of a two-level full factorial design of experiments.

Based on the literature, available research works suffer greatly from the application of full factorial design to study the effects of synthetic parameters on final physical properties of the produced carbon. More importantly, the lack of modeling is a great deal which can only be satisfied when an experimental design (and preferably a full factorial design) has been first developed. Moreover, the best full factorial design should be both cost-(and time) effective and should be able to adequately identify the curvature in the final model response surface. Three-level design of experiments has been frequently used to investigate possible curvature in the final models.

The effect of each individual parameter on the final porous structure not only depends on the studied conditions but also on the nature and origin of the carbon precursor. Based on the reported results in the literature, a separate thorough probe into the effects of synthetic parameters is always required once a new carbon precursor is identified.

Experimental

Carbon precursor preparation and chemical reagents

Used cigarette filters were collected from five different heavy smokers of the same cigarette brand during 8 weeks until enough filters were gathered. Then the filters were all unwrapped from within the cigarette paper and were thoroughly mixed together for future studies.

All chemical were of analytical grade and were used in the experiments as received. In all experiments, ultra-pure water, supplied by an ultra-pure water machine (Millpore Co.) was used.

The details of all the chemicals used have been tabulated in Table 1.

All the glassware including beakers, volumetric flasks and, etc. were provided by Nice or Schott Co. Prior to the experiments, the glassware was thoroughly soaked in 10 %

Table 1 Chemicals used in the experiments

Chemical/details	Brand	Purity (%)
NaOH	Systerm	99
KOH	Sigma-Aldrich	85
KNO_3 (potassium nitrate)	Sigma-Aldrich	99
Na_2CO_3 (sodium carbonate)	Sigma-Aldrich	99
$NaHCO_3$ (sodium bicarbonate)	Sigma-Aldrich	99.5
HCl (hydrochloric acid)	Sigma-Aldrich	37

nitric acid solution overnight (Bhole and Ramteke 2011). The glassware was then completely rinsed several times with tap water and ultrapure distilled water, respectively.

Pyrolysis procedure

In all carbonization experiments a horizontal furnace (Carbolite Co.) with a stainless steel tube was used. The cylindrical steel tube had a diameter of 50 mm and a length of 90 mm.

The carbonization operational parameters (i.e. pyrolysis temperature, hold time and heating rate) were all simply adjusted by the available programmable furnace. Temperature was studied at the three levels of 800, 900 and 1,000 °C. Heating rate was adjusted at 3, 5 and 10 °C/min while soaking time was studied at the values of 0.5, 1 and 3 h. The nitrogen flow into the furnace was provided by a nitrogen tank placed next to the furnace. The flow of the gas was also controlled using an N_2 flow meter (InFlux-Co.). In all experiments the nitrogen gas flow rate was adjusted at a constant value of 100 cm^3/min.

Used cigarette filters (15 g) were initially placed in a crucible and then the furnace tube. The furnace tube was next sealed and nitrogen gas was passed through the furnace tube for 30 min to make sure that the tube was almost free of any trapped oxygen molecules. The filters were next heated at prescribed furnace conditions. The furnace was kept closed with the same flow of nitrogen gas overnight until after the atmospheric temperature was reached. The obtained charred carbon was then removed from the furnace, ground and sieved to a mesh size of 80 to represent carbon in its powdered state. They were then washed several times with hot distilled water and dried overnight in an oven at 105 °C and were kept in a desiccator for future experiments. After each run, the furnace tube was carefully removed from the furnace, completely washed initially with acetone and then with hot distilled water. The washed tube was next heated in the air to make sure that the entire remaining residue was burned off from the tube surface before launching the subsequent run.

Design of experiments

To investigate the effects of carbonization conditions on BET surface area, all controllable and possibly influential process parameters were initially identified. These included carbonization temperature, soaking time and heating rate. To construct an approximation model that can capture interactions between all design variables, a full factorial approach (Montgomery and Runger 2011) may be necessary to investigate all possible combinations. A factorial experiment is an experimental strategy in which design variables are varied together, instead of one variable at a time.

Minitab 16 software was used to design a full factorial arrangement of experiments in a completely randomized design (uniform distribution of errors within all runs) to study the effects of pyrolysis parameters on the BET surface area of the final charred carbon. Also, microporous area has been calculated based on the **t-plot approach. Table 2 has tabulated the full factorial design of experiments and the corresponding values of the response (BET surface area).

Characterization

Nitrogen adsorption–desorption experiments

To evaluate the porous characteristics of the active carbon, adsorption–desorption experiments using liquid nitrogen were performed on a Micromeritics surface analyzer (ASAP 2020). In these experiments, 0.05–0.1 g carbon sample was carefully weighed using a digital balance (Mettler Toledo Co, AB204-S/FACT) and was added to the instrument's sample tube. The sample was initially degassed for 6 h at 200 °C with a heating rate of 1 °C/min to make sure that no residual gas molecule was trapped inside the carbon pores. Next, the saturation and analysis vessels were both carefully filled with liquid nitrogen and then placed into the machine. The ASAP machine was then operated to analyze the sample for its porous structure properties during which the sample pores were filled with nitrogen until saturation pressure was reached. BET and t-plot equations were used to calculate the porous surface area. Pore size distribution (PSD) was calculated by applying Barrett–Joyner–Halenda (BJH) equation to the adsorption branch of the nitrogen adsorption isotherm. Non-local density functional theory (NLDFT) model has also been applied for the calculation of PSD for comparison. In this method, either argon or nitrogen can be used. However, our instrument (ASAP 2020) used liquid nitrogen (77 K) to calculate PSD based on both BJH and NLDFT models. The software was capable of applying NLDFT model to the porous carbon materials to successfully cover both micro and mesoporous regions.

Scanning electron microscopic (SEM) analysis

To investigate the surface morphology of the produced carbon, SEM analysis (FEI Co, Quanta 400F FESEM) was

Table 2 Full factorial design of experiments and corresponding BET and microporous surface areas with carbon yield

Experiment	Temperature (°C)	Heating rate (°C/min)	Soaking time (h)	Carbon yield (%)	BET surface area (m^2/g)	Micropore area (m^2/g)
1	800	3	3	15	487	309
2	800	10	3	15	421	259
3	1,000	3	3	15	376	220
4	800	10	1	15	408	236
5	900	3	1	15	448	283
6	900	5	0.5	15	531	301
7	1,000	3	1	15	418	257
8	900	10	0.5	14	414	246
9	900	3	0.5	15	432	281
10	1,000	10	3	15	347	189
11	800	5	0.5	14	457	270
12	800	10	0.5	15	471	262
13	800	5	1	15	484	296
14	900	3	3	15	423	267
15	1,000	5	0.5	15	399	237
16	900	10	3	15	409	255
17	900	5	3	15	597	453
18	1,000	3	0.5	15	446	279
19	1,000	5	1	16	461	284
20	1,000	5	3	16	559	388
21	800	3	0.5	16	424	270
22	800	3	1	15	467	285
23	900	10	1	15	398	217
24	800	5	3	16	453	278
25	1,000	10	1	15	366	199
26	1,000	10	0.5	16	344	197
27	900	5	1	15	563	341

used. The SEM was operated at an accelerating voltage of 20 kV in an either low or high vacuum mode, depending on the nature of the sample to be analyzed. Prior to any analysis, the samples were dried at 373 K and were then stored in a desiccator overnight. In the experiments, a small portion of sample was placed on a small carbon tape which was next placed on an aluminum platform in the microscope.

Energy dispersive X-ray spectroscopy analysis (EDX)

An energy dispersive X-ray spectroscope (Oxford Instruments Co. X-Max) coupled with SEM, was used in the EDX analyses. Sample preparation was identical to that of SEM analyses. EDX makes it possible to detect the elemental composition of any matter being studied. EDX elemental composition could be quantitatively stated in weight percentage or atomic percentage. It is possible to use EDX to study only a particular area as small as a few nanometer diameters.

Thermal gravimetric analysis (TGA)

To investigate the thermal decomposition behavior and proximate analysis of the used cigarette filter and synthesized carbon a thermal gravimetric analyzer (Mettler Toledo Co, Star System) was used. The analyzer was connected to oxygen and nitrogen gas capsules which could be separately controlled. A very small amount of sample was placed into a 150 µl alumina crucible which was then placed inside the instrument. The TGA started the operation by the introduction of the relevant gas into the sample chamber.

Fourier transform infrared spectroscopy (FTIR)

To investigate the surface functional groups on the synthesized carbon a Fourier transform infrared spectroscope (Nicolet DXc20 FTIR) was used. Initially samples of active carbon were oven dried overnight at 383 K. The already dried powder was next finely mixed with KBr at a ratio of 1:100. FTIR spectra were obtained at a resolution of cm^{-1}. The FTIR spectroscope scanned the carbon sample with 200 scans per second while having an aperture setting of 15. Water vapor was used as the background spectra and for each sample, this background spectra was subtracted from the recorded spectrum.

Surface chemistry analysis (Boehm titration)

To investigate the amount of acidity and basicity of the carbon surface, Boehm titration was used. The carbon sample

was initially degassed at 150 °C to make sure no physically trapped gases nor had vapors remained inside the porous structure. First, the solutions of Na_2CO_3 (0.1 N), $NaHCO_3$ (0.1 N), NaOH (0.1 N) and HCl (0.1 N) were prepared. 0.1 g of carbon sample was placed in a 50 ml of the above solutions which was kept in a capped glass. The glasses were then placed on a shaker for a duration of 72 h. After the contact period was passed, the solutions were filtered and 10 ml of each solution was taken for the subsequent titration. The filtration procedure was quite sensitive and was done with extra care. The titration was complete when solution pH reached the value of 7. The filtrates were then ready for titration with NaOH (0.1 N) and HCl (0.1 N). HCl volume consumed for the titration of NaOH, Na_2CO_3 and $NaHCO_3$ solutions was measured to estimate the acidic strength. The basic strength was determined by measuring NaOH volume consumed for the titration of HCl. All experiments were run in triplicates (Malekbala et al. 2012).

Result and discussion

Properties of the raw carbonaceous material (used cigarette filter)

The investigation of certain properties of the raw carbonaceous material (prior to carbonization) is a necessary step to decide whether the initial matter would be a decent potential candidate for the production of active carbon. The investigation procedure is known as proximate analysis.

Proximate analysis

To study the initial carbonaceous material, i.e., used cigarette filter in terms of carbon content, moisture content, volatile content and ash content, proximate experiments were conducted. During the process (Lua et al. 2004), the sample was heated in nitrogen (inert) atmosphere from room temperature to 110 °C and was kept at this temperature for 1 h for the moisture content to be eliminated and determined. Then the temperature was raised to 850 °C and was maintained at this temperature for 7 min. The weight loss after this time was an indication of the volatile matter in the used cigarette filter sample. The temperature was then cooled down to 800 °C. At this point, the atmosphere was shifted to oxygen gas (an oxidizing agent). The temperature was maintained constant until a constant weight was observed. The remaining matter was indicative of the total ash content of the raw material. Also, the weight loss during this stage is understood to be the fixed carbon content in the raw matter. The TGA graph obtained through the proximate analysis is shown in Fig. 1.

Based on this graph, the proximate analysis results have been tabulated in Table 3.

According to the proximate analyses, the initial matter has a high amount of volatile matter. This can facilitate the development of porosity within the charred carbon (Rodriguez-Reinoso and Sepulveda-Escribano 2001). Used cigarette filters also proved to have a small content of ash. This is an advantage for a carbon precursor (Rodriguez-Reinoso and Sepulveda-Escribano 2001). These two features of the used cigarette filters are favorable properties for the preparation of activated carbon (Lua et al. 2004). However, the amount of fixed carbon after the TGA experiments showed to have a low value which is still satisfactory compared to other initial materials mostly with agricultural origins, used in the production of activated carbons.

Scanning electron microscopy

The morphology of the starting material (used cigarette filter) is firstly investigated prior to the carbonization process. The SEM image of used cigarette filter is shown in Fig. 2. Figure 2 can clearly show that the carbon precursor consists of numerous bundles of Y-shaped head cellulosic fibers in a completely random fashion.

Energy dispersive X-ray spectroscopy

To study the regional elemental compositions of the raw carbonaceous material, EDX analysis was applied. Figure 3 represents the EDX spectrums of used cigarette filter. Table 4 has tabulated the compositional analysis of used cigarette filters.

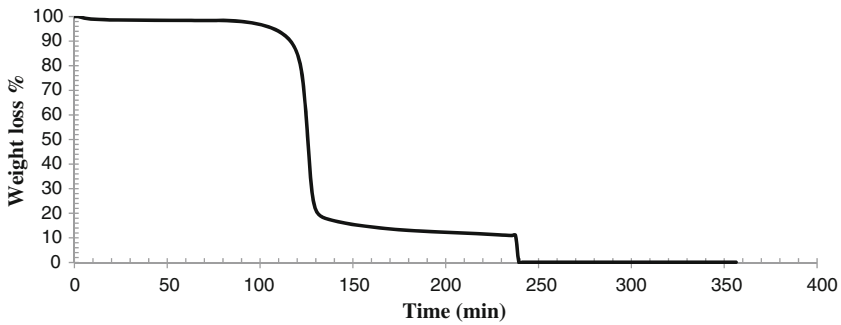

Fig. 1 The TGA graph produced as a result of proximate analysis of used cigarette filter

The values may not only contribute to the filter material but also to the cigarette smoke constituents trapped throughout the filter. The metals detected in cigarette filters can originate from the additives which are regularly added to tobacco. Potassium is added to tobacco as potassium sorbate. The presence of titanium can also be attributed to titanium dioxide which is another tobacco additive in the industry (Fowles and Bates 2000). However, it is noticeable that elemental carbon is the main chemical element used in cigarette filters, making up for around 60 wt% of total raw material with elemental oxygen being the runner-up with a value of around 40 wt%.

Graphical illustrations

Graphical plots are useful ways to interpret the effects of control variables (independent variables) on the response (dependent variable). These illustrations can be categorized into two main classes: main effects plots and interactions effects plots. Main effect plots show the overall effects of one factor on the response value. However, main effect plots can be validated only if there is little interaction among the studied parameters. The analysis of the results by Minitab 16 showed little interactions among pyrolysis temperature, heating rate and soaking time. Thus, it is more straight forward to directly study the main effects of the pyrolysis parameters on the porous surface area of the charred carbon.

Table 3 Proximate analysis of used cigarette filter (w %)

Moisture (%)	Volatile matter (%)	Fixed carbon (%)	Ash (%)
1.608	87.240	11.056	0.096

Effect of carbonization temperature on BET surface area

The investigation of the effect of carbonization temperature on BET porous surface area is presented in Fig. 4. The graph shows that the BET surface area increases by around 15 % from 436 to 500 m^2/g when temperature increases from 800 to 900 °C. This can be attributed to the fact that an increase in temperature may result in an increase in the amount of volatiles being released from inside the carbon network and decomposition of major compounds of cigarette filter, i.e., cellulose acetate, at elevated temperatures (Bouchelta et al. 2012). Also, blocked pores filled with tar-like materials during the carbonization process may be unblocked when temperature increases. These two phenomena can modify porous carbon network in a way that a modified porous media will be created. However, when carbonization temperature is further

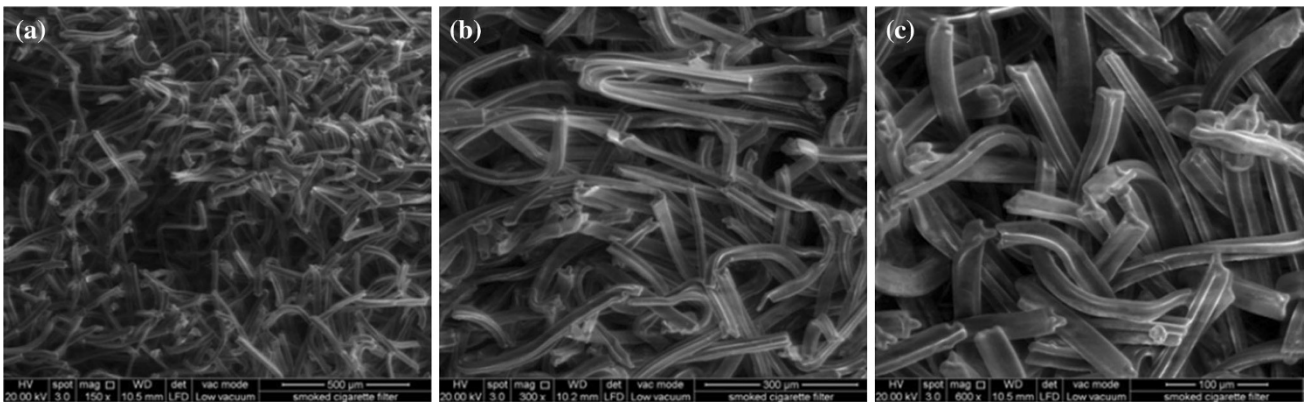

Fig. 2 SEM images of used cigarette filters in three different magnifications: **a** ×150, **b** ×300, **c** ×600

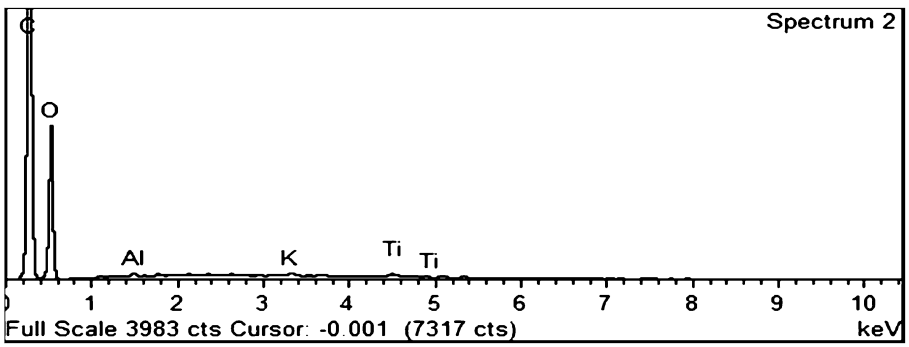

Fig. 3 EDX spectrum of used cigarette filter

Table 4 EDX elemental analysis of used cigarette filter

Element	Wight %	Atomic %
C	59.22	66.07
O	40.30	33.76
Al	0.11	0.05
K	0.13	0.05
Ti	0.24	0.07

increased, the porous surface area decreases. This trend has been also observed by other researchers. Lua et al. (2004) reported the same increasing pattern in BET surface area of char obtained through the pyrolysis of pistachio nut shells. The BET surface area increased from 333 to 778 m^2/g (around 134 %) when pyrolysis temperature was elevated from 250 to 500 °C. Identically, the effect of temperature on BET surface area of the final char was also studied by Bouchelta et al. (2012). They confirmed the same effects when date pits were carbonized between 500 and 700 °C. In their study BET surface area increased from 50 to 297 m^2/g (494 %). It is observed that BET surface area decreases by 20 % when carbonization temperature is further increased from 900 to 1,000 °C. This may be caused by the decomposition and subsequent softening of some volatile fractions to form an intermediate melt in the char structure (Lua et al. 2004). This melt can easily block the pores and decrease the total surface area. Fu et al. (2012) studied specifically the effect of temperature on final BET surface area for four different agricultural residues, i.e., maize stalk, rice straw and cotton straw. They consistently reported the same increasing–decreasing pattern as compared to our results. It is noticeable that chars obtained through the pyrolysis of cigarette filter, rice straw and cotton straw all have a very similar way of decomposition pathway at temperatures of 800, 900 and 1,000 °C. The BET surface areas for all these chars begin to decline at a temperature of 900 °C. This may be due to the fact that all these materials are from a cellulosic origin and therefore, their decompositions can potentially follow the same route.

Effect of soaking time on BET surface area

The investigation of the main effect of soaking time on BET porous surface area is presented in Fig. 5. As expected, the longer soaking time has resulted in an increase in BET surface area due to the increased release of volatile matter. However, this effect is more severe when the hold time has increased from 0.5 to 1 h. During this period, the major structure of surface area has been developed. The effect is less pronounced when soaking time has increased from 1 to 3 h although the porous surface area is still increasing as seen by the milder slope of the line from 1 to 3 h of soaking time. Bouchelta et al. (2012) while observing the same trend

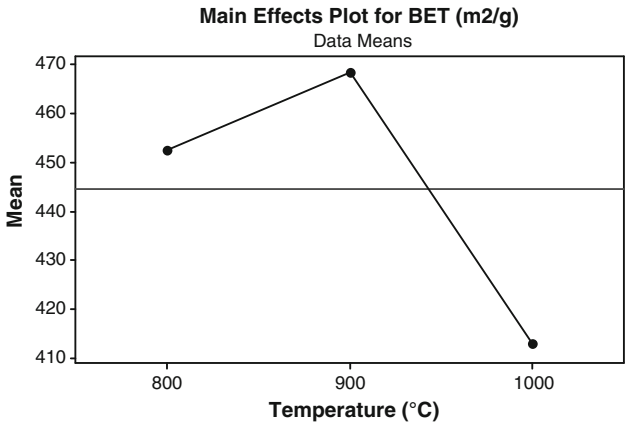

Fig. 4 Effect of carbonization temperature on BET porous surface area

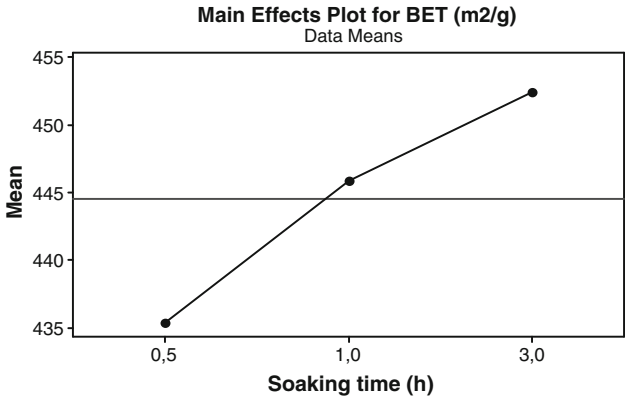

Fig. 5 Effect of soaking time on BET porous surface area

emphasized the fact that further increase in soaking time (to 4 h and more), though may increase the BET surface area to a lesser extent, it would not be energetically wise in terms of the amount of heating costs. Also Lua et al. (2004) reported that in the pyrolysis of pistachio nut shells, increasing hold time from 2 to 2.5 and 3 h lowers the BET surface area. They concluded that prolonged heat treatment leads to an increase in softening of some volatile fractions (similar to the temperature effect) and forms an intermediate melt which seals off some pores.

Effect of heating rate on BET surface area

The investigation of the main effect of heating rate on BET porous surface area is presented in Fig. 6. The results show an increase in BET surface area when heating rate has increased from 3 to 5 °C/min. The porous area has then decreased when heating rate has been further elevated. The dependency of porous surface area and heating rate can be explained by considering the heat and mass transfer resistances. At lower heating rates, the nitrogen molecules do

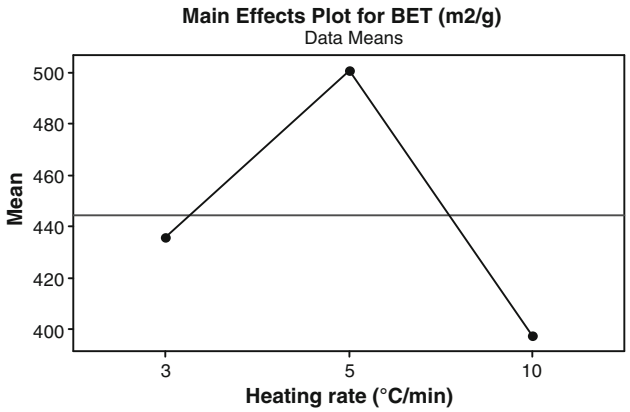

Fig. 6 Effect of heating rate on BET porous surface area

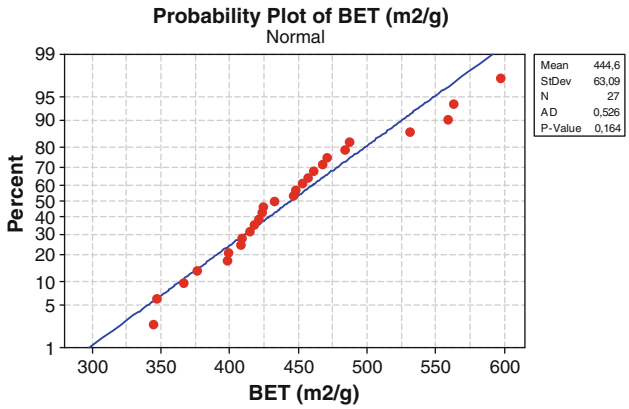

Fig. 7 Normality test plot for BET surface area

not have enough energy to diffuse thoroughly into the porous structure of carbon network. Thus, their interactions are confined to the surface of the carbon and/or regions in close proximity to the carbon surface. By increasing the heating rate, the temperature elevation rate inside the cellulose-based filters and char is brought about more quickly. Consequently, this results in an enhanced extraction of volatile compounds and alternatively an enhancement in the decomposition of cellulose-based materials. By deeper penetration and more intensive diffusion of nitrogen molecules into the raw material and char, more surface area will be created (Bouchelta et al. 2012). On the other hand, when heating rate is increased to 10 °C/min, higher temperature will be reached inside the material. Bouchelta et al. (2012) observed that by increasing heating rate from 10 °C/min to higher rates, partial graphitization followed by the creation of grapheme structure occurs in the pyrolysis of date pits. They highlighted that this graphitization is not in favor of porous surface area development. Same trend has also been reported by Lua et al. (2004).

Analysis of variance (ANOVA)

ANOVA assesses the average (main effect) contribution of each input factor (parameter) to the overall outcome variance, i.e., to the sum of the squared differences between each simulation and the overall mean. It can also assess the interactions between factors. In ANOVA, each factor takes a limited number of distinct values (the levels). ANOVA is flexible with respect to the number of levels of the input factors, and can cope with quantitative as well as qualitative factors (Ginot et al. 2006). Prior to applying ANOVA to investigate which factor pose a significant effect on the response, i.e., BET surface area, the response values must pass the normality test. Figure 7 illustrates the result of the normality test. Since the data have a p value of larger than 0.05, i.e., 0.164, we can conclude that our response data is normal and ANOVA can be applied for further analyses.

The results of the ANOVA for BET surface area by applying balanced ANOVA technique have been tabulated in Table 5.

According to the results and p value of the ANOVA analysis, the factor with significant effects on the response (BET surface area) is heating rate (with a p value <0.05). However, temperature also shows a p value very close to the critical value of 0.05, i.e., 0.052. This nominates temperature as a potential contributor to the BET variations. This needs to be further investigated by applying statistical plots in the next section. It seems that soaking time (with a p value of 0.683) does not play an important role in the variation of BET surface area. Two-way interactions, i.e., temperature versus soaking time; soaking time versus heating rate and temperature versus heating rate (all with a p value >0.05) also show insignificant effects on the BET variations. The final R-Sq (R^2) value (87.06 %) implies that the chosen factors (temperature, soaking time, heating rate) contribute to 87.06 % of the variations in BET values. It means that 12.94 % of the variations have been due to unknown (uncontrollable) effects.

RSM in modeling BET surface area with all significant factors as model parameters

To draw a comparison between the accuracy of the model developed with all the significant variables which were previously determined by means of ANOVA, i.e., carbonization temperatures and heating rate, four models have been developed by applying surface response method. The models descriptions and their corresponding R^2 values are tabulated in Table 6.

Based on the RSM model fit values, the worst fit has been achieved when a first-degree polynomial is passed through the design points (linear RSM model). By applying the linear model together with the addition of interactions terms, the R^2 value has slightly improved by around 9 % from 22.59 to 24.69 %. This improvement although is in

Table 5 Table of the analysis of variance (ANOVA) for BET surface area of charred carbon

Factors	Type	Level	Values
Temperature (°C)	Fixed	3	800; 900; 1,000
Soaking time (h)	Fixed	3	0.5; 1; 3
Heating rate (°C/min)	Fixed	3	3; 5; 10

Source	DF	SS	MS	*F*	*p*
Analysis of variance for BET (m^2/g)					
Temperature (°C)	2	14674	7,337	4,38	0.052
Soaking time (h)	2	1342	671	0,40	0.683
Heating rate (°C/min)	2	48704	24,352	14,54	0.002
Temperature (°C) × soaking time (h)	4	594	148	0,09	0.983
Soaking time (h) × heating rate (°C/min)	4	7940	1,985	1,19	0.387
Temperature (°C) × heating rate (°C/min)	4	16842	4,211	2,51	0.124
Error	8	13396	1,675		
Total	26	103491			
$R^2 = 87.06$ %					

Table 6 Four different RSM model parameters and their corresponding R^2 values

Model name	Model parameters	Model R^2 value (%)	Model R^2 prediction value (%)
Linear	Temperate, heating rate	22.59	8.10
Linear plus interactions	Temperature, heating rate	24.69	6.44
	Temperature × heating rate		
Linear plus squares	Temperature, heating rate	61.24	41.62
	Temperature squared		
	Heating rate squared		
Full quadratic	Temperature, heating rate	63.35	41.46
	Temperature squared		
	Heating rate squared		
	Temperature × heating rate		

favor, however, the reduced prediction R^2 is a drawback of the second design. When interactions are taken out from the model and are replaced with the factor squared terms, noticeable improvement in R^2 value as well as prediction R^2 has been observed. This is a reasonable indication of the presence of curvature in the model surface. When the most complex scenario of the RSM design is applied, i.e., full quadratic approach, a slender growth in R^2 value has been observed. This is in favor of the optimum RSM design. It is mentionable that albeit a minor reduction in prediction R^2, this change is insignificant compared to the more noticeable increase in the model R^2 value. Based on the above discussion, the optimum RSM is understood to be a full quadratic model.

The wire-frame 3D plot of the optimum RSM and the corresponding contour plot are shown in Figs. 8 and 9, respectively.

The expected curvature and its intensity can be readily observed in Fig. 8. However, this surface can be studied in a different view by projecting its surface onto a plane surface beneath. By doing so, Fig. 9, conventionally known as contour plot, is formed. In this plot lines of constant response are drawn on an *x*–*y* plane with each axis corresponding to one factor level. In contour plots, each line simply represents a single height in the surface graph. The advantage of contour plots is the capability of investigating the levels of factors which result in changes in the shape or height of a response surface (Montgomery and Runger 2011). The full quadratic model coefficients corresponding to the optimum model surfaces above have been tabulated in Table 7.

Based on the coefficient, the final model second-degree polynomial function is:

$$y = -2664.03 + 6.45a + 126.56b - 7.57b^2 - 0.04(ab)$$

where y = BET surface area (m^2/g), a = carbonization temperature (°C) and b = carbonization heating rate (°C/min).

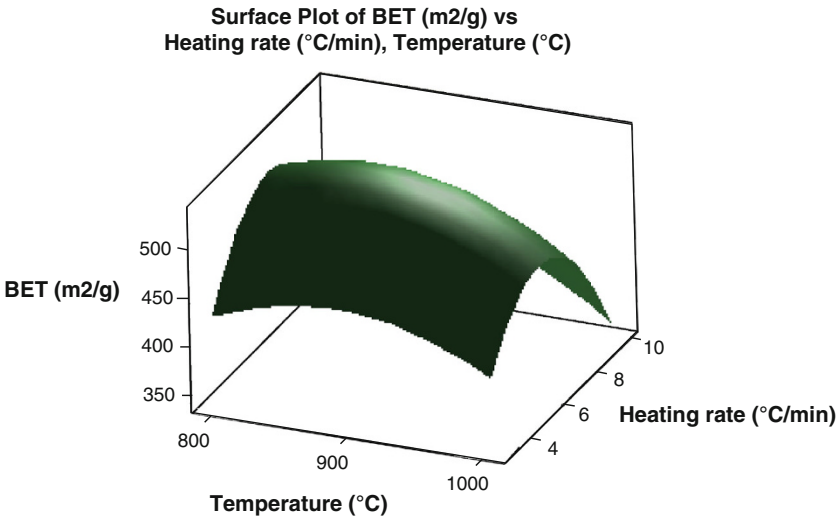

Fig. 8 Full quadratic RSM model surface

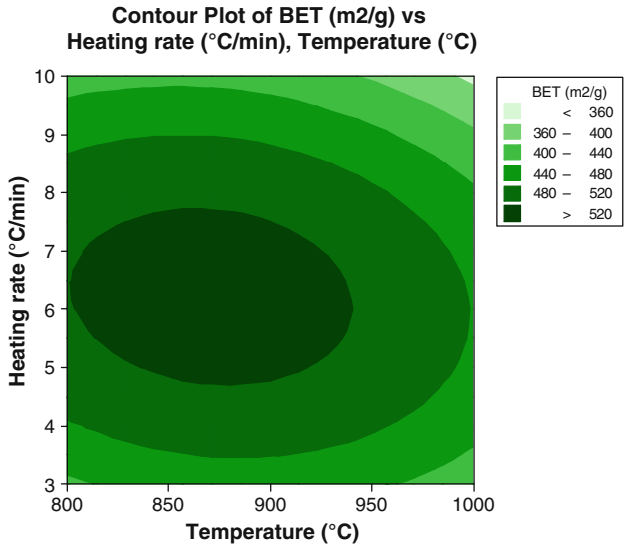

Fig. 9 Full quadratic RSM model contour plot

Table 7 Full quadratic RSM model coefficients

Full quadratic RSM model parameter	Coefficient	*p* value
Constant	−2,664.03	0.073
Temperature (°C)	6.45	0.052
Heating rate (°C/min)	126.56	0.004
Temperature × temperature	0.00	0.052
Heating rate × heating rate	−7.57	0.000
Temperature × heating rate	−0.04	0.285

Characterization of charred carbon

The charred carbon produced at 900 °C, 3 h of soaking time and 5 °C/min heating rate (optimum conditions) has been characterized for its physical as well as chemical properties.

TGA of charred carbon during the production

It was observed that the cellulose-based cigarette filter turns into a black matter after the heat treatment in complete. This black matter is completely different in appearance from the initial raw material. The final product is brittle and can be easily crushed into powder. The carbonization process leading to the decomposition of the raw material and yielding the final product with the maximum BET surface area was first studied by mean of a thermal gravimetry analyzer. The decomposition and weight loss trends are graphed in Fig. 10.

The graph shows that the major weight loss due to the decomposition of cigarette filter constituents is between the temperatures of around 200 and 380 °C. During this period a weight loss of around 80 % can be observed. This is as a result of the continuous dehydration and removal of acetic acid from the filters (Polarz et al. 2002). From this point forward until the temperature of approximately 500 °C is reached, another weight loss of around 5 % is measured. This can be due to an incomplete carbonization of raw material (Polarz et al. 2002). The final carbon yield as estimated is the recorded to be around 15 %. This is in satisfactory agreement with the values reported in the literatures (Laszlo et al. 2000). From this temperature beyond and in prolonged soaking times, no significant weight loss was detected.

Proximate analysis of charred carbon

Proximate analyses including total moisture content, total volatile matter content, fixed carbon and total ash content were conducted to evaluate the quality of the optimum carbon sample (corresponding to maximum BET porous surface area). All experiments were carried out in

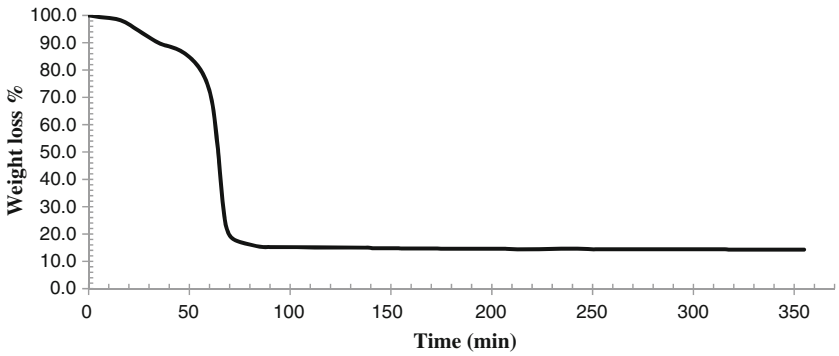

Fig. 10 Decomposition of the cigarette filter under optimum carbon sample production conditions

Table 8 ASTM standards for activated carbon and their designations (ASTM International 1996–2012)

	ASTM standard for activated carbon designation
Total moisture content	D 2867-99
Total volatile matter content	D 5832-98
Total ash content	D 2866-94 (reapproved 1999)

accordance with the final version of the American Society for Testing and Materials (ASTM) guideline, released in the year 2000. Specifically, the experiments for carbon sample were done based on ASTM standards for activated carbon. These standards have been tabulated in Table 8.

Prior to the proximate experiments, carbon sample was washed with 0.1 M HCl solution to remove surface ash. Next, the carbon was washed with ultrapure water to remove the hydrochloric acid and dried in a vacuum drying oven at 150 °C overnight (Tao and Xiaoqin 2008).

During the proximate analysis, the carbon sample was heated up to 150 °C and was maintained at this temperature until a constant weight was observed (3 h is usually sufficient). Then, the sample was heated to 950 °C and was kept at this temperature for 7 min. Next, the sample was cooled down to 650 °C while an oxidizing gas (oxygen) was introduced into the sample chamber. The sample remained at this temperature under the constant flow of oxygen gas until no further mass change was recorded (It normally takes between 3 and 16 h). The difference between the final ash and the sample weight before the oxidation began represents the total fixed carbon.

Table 9 tabulates the proximate analyses values of the charred carbon. The amount of fixed carbon is calculated by subtracting the weight loss right after the removal stage of volatile matter from the final weight (total ash content).

A value of 73.74 % of fixed carbon indicates a relatively good degree of carbon matter compared to other charred waste matters. The amount of remaining ash in the final carbon product owes to the presence of various metals such as Al, K and Ti which were initially detected using EDX. The relatively moderate value of ash, though still

Table 9 Proximate analysis of charred carbon (w %)

Moisture (%)	Volatile matter (%)	Fixed carbon (%)	Ash (%)
1.24	6.56	73.74	18.46

comparable with charred matter obtained from other wastes, needs to be paid careful attention when this carbon is aimed to be used in sensitive water treatment systems. This is due to the fact that the ash trapped within the carbon network can itself pose a secondary pollution into the water.

Porous structure of the optimum carbon sample

Nitrogen adsorption–desorption experiments have been long used to investigate the porous nature of active carbons and porous properties of solids due to its simplicity and accuracy. The adsorption–desorption isotherm of the optimum carbon sample is shown in Fig. 11.

The shape of the isotherm demonstrates a type IV standard isotherm curve which is an indication of strong interaction between the adsorbent and adsorbate molecules. Moreover, type IV isotherm confirms the presence of mesopores within the carbon porous network. Adsorption by mesoporous matters is almost always associated with a hysteresis loop which is seen between the adsorption and desorption branches of the isotherm. The hysteresis is developed as a result of a mechanistic difference between the capillary condensation of adsorbate into the mesopores (pore filling mechanism) and mesopores emptying (Marsh and Rodriguez Reinoso 2006). The hysteresis loop is a consequence of the continuous condensation of adsorbate molecules in the pores during the adsorption process which accompanies the creation of a meniscus. The vapor pressure right above the meniscus decreases as the pore size decreases. This is because of the smaller curvature radius. Consequently, molecules in the smaller pores tend to be desorbed last with a constant reduction in vapor pressure (Rodriguez-Reinoso and Sepulveda-Escribano 2001). The characteristics of this type of materials provide that there must exist a contacting point at the end of the pore space. The contacting spot and the area adjacent to it would

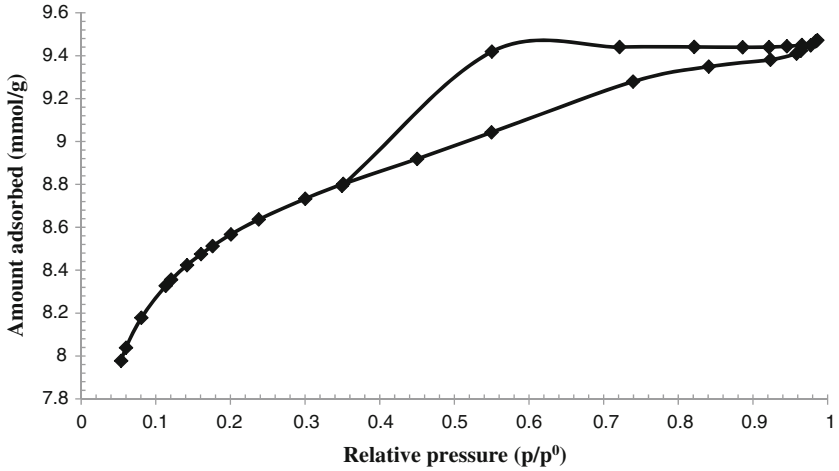

Fig. 11 Nitrogen adsorption–desorption isotherm

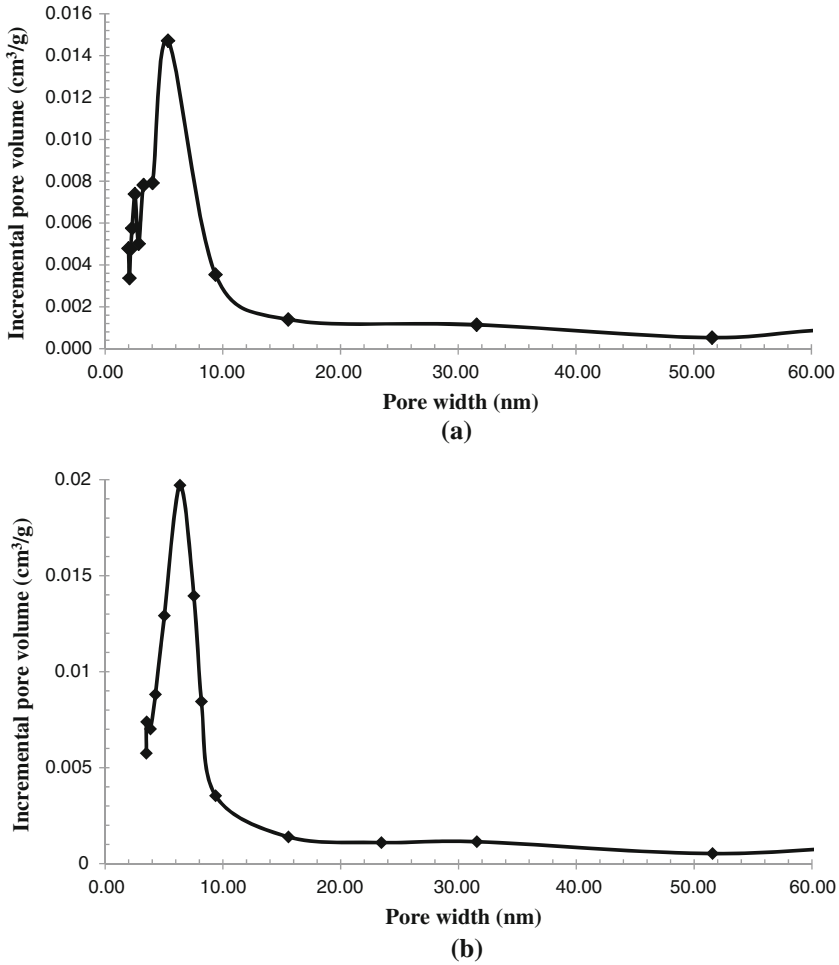

Fig. 12 Pore size distribution graphs: **a** BJH model based on adsorption branch of isotherm, **b** NLDFT model with nitrogen at 77 K

provide a condition within which a nucleus can begin developing and thus condensation is initiated (Nogi et al. 2012). The hysteresis in Fig. 11 is clearly an H_2 class of hysteresis. H_2 type of hysteresis is an indication of the interconnection of pores though the narrower spaces of the particle or the network of pores is developed by connecting necks. Consequently, the adsorption remains in an equilibrium status. However, the previously explained ink-bottle effect leads to the formation of hysteresis along which the condensate is not able to evaporate unless the vapor pressure drops down to a value corresponding to the neck size. As a result, the hindered evaporation volume along this path fails to effectively represent the pore volumes of the pore size at a specific pressure (Nogi et al.

2012). In addition, the adsorption in macropores is visible in the produced isotherm graph at high relative pressures where $p/p^0 \rightarrow 1$. This is confirmed by the sudden increase in adsorption at a quantity near relative pressure of unity (Polarz et al. 2002).

The isotherm, however, needs to be finally interpreted in a quantitative manner so that a decent judgment can be drawn. It has been desired to associate a single number to each carbon, i.e., the total porous surface area as a quantitative label. By applying the BET equation to the isotherm in Fig. 11, a total surface area (including micro and meso pores) of 597 m^2/g has been calculated.

There is a need to know not only how much porosity exists within a carbon network but also equally the quality of the developed porosity counts. The quality of the structure of the porosity is determined by PSD (Marsh and Rodriguez Reinoso 2006). PSD of the charred carbon is shown in Fig. 12.

The size distribution of mesopores can be calculated from the hysteresis loop as explained by Gregg and Sing (1982) using computational techniques. In addition, the BJH method has been widely accepted to calculate the PSD in porous carbon materials. Although there has been a long discussion upon which branch of hysteresis must be analyzed to calculate PSD using BJH approach, however, some understandings have been suggested. When H_2 hysteresis types are formed, the adsorption branch of the isotherm should be considered for the calculation of PSD (Nogi et al. 2012). Based on Fig. 12a, there exist pores within the mesoporous region (2–50 nm) due to the expansive bell shape of the PSD graph from around 2 to 10 nm. Although mesoporosity is extended to pores with wider pore widths to even beyond 20 nm, however, this region does not contribute much to the available mesopores. The PSD also indicates that there even exists macroporosity within the carbon network as the PSD graph continues to grow to the values beyond 50 nm also. The average pore width calculated by applying BJH model to the adsorption branch of the isotherm is 3.3209 nm. Figure 12b illustrates the PSD calculated based on NLDFT. This is a more modern method in the calculation of PSD compared to conventional BJH. There exists a shift of PSD graph to the right in Fig. 12b. This kind of shift has been similarly reported by Ojeda et al. (2003). It is now known that BJH model, if compared to NLDFT model or electron microscopy, reveals pore sizes smaller than the real ones by as much as several tens of Å. A comprehensive theoretical description, comparing BJH and NLDFT methods can be found in the literature (Ojeda et al. 2003).

The total pore volume is calculated based on single-point total pore volume method at a relative pressure of 0.98. Table 10 has tabulated the calculated values for the structural porous properties of the charred carbon.

The most popular activated carbons possess a pore volume in the range of 0.2–0.6 cm^3/g with a surface area between 800 and 1,500 m^2/g (Rodriguez-Reinoso and Sepulveda-Escribano 2001). Based on these facts the synthesized carbon shows acceptable value for the pore volume.

Table 10 Physical properties of the charred carbon

Total surface area (m^2/g)	Micropore area (m^2/g)	Mesopore area (m^2/g)	Total pore volume (cm^3/g)	Micropore volume (cm^3/g)	Average pore diameter (nm), BJH
597	453	144	0.33	0.23	3.32

SEM analysis

The SEM image taken from the surface of the non-modified carbon is shown in Fig. 13. Since carbon materials are known as conductive materials, the SEM analyses for carbon samples were conducted under the high vacuum mode. The images are taken at two separate magnifications.

These images can clearly reveal the surface morphology of the surface of carbon which is thoroughly different from that of the raw material. It can be seen that the surface is comprised of giant macro pores. These macropores can

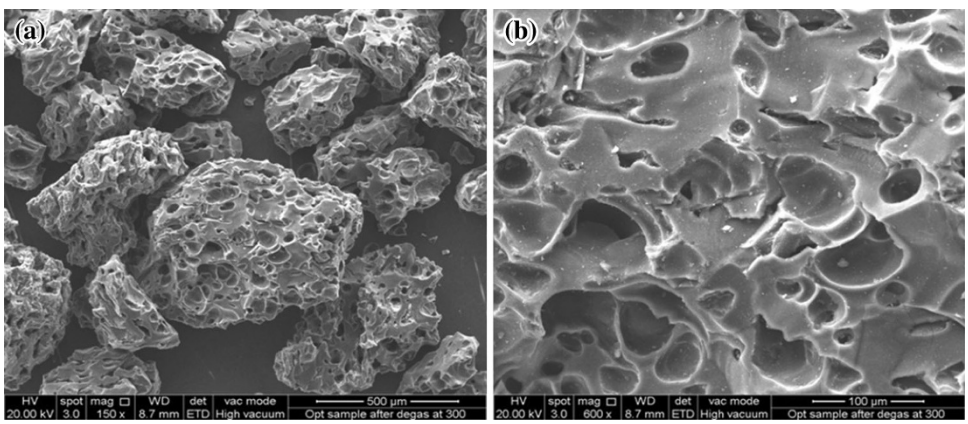

Fig. 13 SEM images taken from the surface of charred carbon at two magnifications: **a** ×150, b ×600

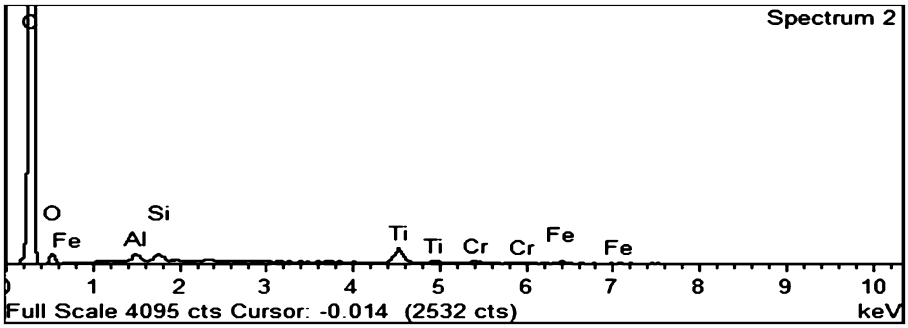

Fig. 14 EDX spectrum taken from the surface of optimum charred carbon

Table 11 EDX elemental analysis of charred carbon

Element	Weight %	Atomic %
C	89.92	94.05
O	6.11	4.80
Al	0.36	0.17
Si	0.36	0.16
Ti	2.31	0.61
Cr	0.31	0.08
Fe	0.61	0.14

play a determining role in transferring the adsorbate and thus can alternatively affect the kinetics of reaction happening inside these pores. The presence of macro pores was earlier confirmed by the sudden increase in the adsorption quantity of nitrogen in the isotherm when $p/p^0 \rightarrow 1$. The presence of macropores is essential in the activated carbons which are used in liquid phase application (Rodriguez-Reinoso and Sepulveda-Escribano 2001). It is seen that the surface openings have not been blocked at the carbonization temperature of 900 °C by the intermediate melt which is often created at higher temperatures resulting to a decrease in BET surface area. This shows evidence that the 900 °C has possibly been high enough to decompose and evaporate the intermediate melt which can be formed by the condensation of higher molecular weight molecules on the surface of the carbon at lower temperatures.

Energy dispersive X-ray (EDX) analysis

The regional distribution of elements on the surface of carbon particles was determined by the same SEM together with energy dispersive X-ray spectroscopy (Li et al. 2011). The EDX spectrum and the compositional analysis are shown in Fig. 14 and Table 11, respectively.

The EDX spectrum reveals that the produced charred carbon consists mainly of elemental carbon and oxygen. However, the spectrum confirms the presence of several heavy metals as well. Among those, Al and Ti were already detected in raw cigarette filters as a result of the additive added to tobacco such as TiO_2. Moreover, Si, Cr and Fe could have been added similarly to the synthetic carbon. These heavy metals could have been existed as trapped compounds in the cigarette smoke. Chromium has been reported to be detected in cigarette smoke (Fowles and Bates 2000); therefore, its presence in final charred carbon may have originated from the trapped chromium-containing compounds within the cigarette filter layers. Disposed cigarette butt filters and smoked tobacco are the main sources of heavy metals in the cigarette filters. These metals include Al, Br, Cd, Cr, Cu, Fe, Pb, Mn, Ni, Sr, Ti and Zn (Moerman and Potts 2011). The presence of these heavy metals highlights the fact that the synthesized carbon should be used with care and extra caution in water treatment systems.

Surface chemistry of non-modified carbon: Boehm titration

Three different types of carbon–oxygen surface functional groups have been identified as the acidic, basic and neutral. While the acidic surface groups have been successfully classified so far, basic surface oxygen groups have been much less characterized.

These terms have been originated from the fact that when a carbon is brought into equilibrium with pure water, changes in water pH (concentration of H^+ in water) will be observed. If the water pH is <7, it means that the water has been acidic due to the dissociation of H^+ from the acidic surface groups. However, in case of a basic solution, the pH would rise to a value of greater than 7.

There have existed several approaches to evaluate the surface functional groups quantitatively and qualitatively. In this work, Boehm titration was performed to investigate the amount of surface acidity and basicity of the surface of the active carbon (Malekbala et al. 2012). The titration results are shown in Table 12.

The surface acidity of a carbon matter is often quantified by considering its alkaline neutralization capacity during which the alkali cations are exchanged for the hydrogen

Table 12 Boehm titration: quantities of neutralizing chemicals used and total acidity and basicity of the carbon

Na_2CO_3 (ml)	$NaHCO_3$ (ml)	NaOH (ml)	HCl (ml)	Na_2CO_3 (mmol/g)	$NaHCO_3$ (mmol/g)	NaOH (mmol/g)	Basicity (mmol/g)	Acidity (mmol/g)
50.5	58.2	52.7	0.85	0.2382	0.3464	0.6587	0.0116	0.7671

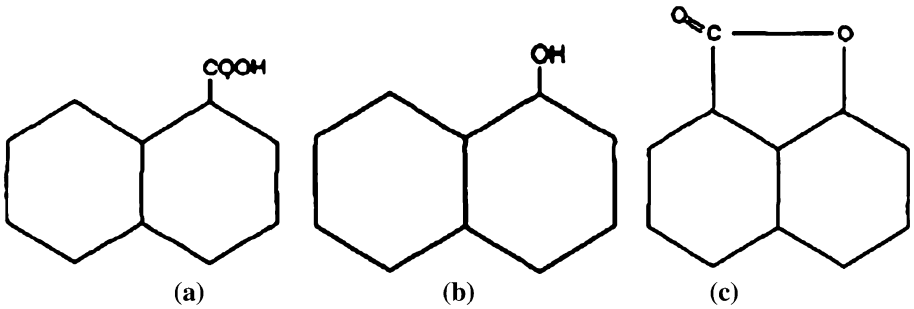

Fig. 15 Acidic surface carbon–oxygen functional groups: **a** Carboxyl, **b** Phenolic, **c** Lactone

Table 13 Acidic functional groups detected by Boehm titration

Carboxylic groups (mmol/g)	Lactonic groups (mmol/g)	Phenolic groups (mmol/g)
0.3464	0.0001	0.4205

ions carpeting the surface of carbon in forms of acidic oxides (Bansal and Goyal 2005). As a general approximation, titration with NaOH and HCl can reveal the degree of surface acidity and basicity based on their corresponding values (Li et al. 2003). In addition, Boehm titration has been effectively applied in detecting and quantifying specific surface functional groups as well. Boehm titration was applied in detecting specific oxygen-functional groups on the carbon surface (Li et al. 2003). Acidic surface functional groups, a class of oxygen complexes, include carboxyl, quinone, carbonyl, lactone, hydroxyl and carboxylic anhydride (Yin et al. 2007). It has been highlighted that the existence of several groups is much more influential than others, i.e., carboxyls, lactones, phenols, quinones and hydroquinones. Based on this fact, in another classification, surface acidity of the carbon surface has been attributed to the presence of carbon–oxygen surface complexes formed as carboxyls, lactones and phenolic groups (Bansal and Goyal 2005). These groups are shown in Fig. 15.

These groups are bound to the edges of the graphite-like layers of carbon (Stavropoulos et al. 2008). It has been established that during the titration process, $NaHCO_3$ titrates carboxyl groups only while NaOH titrates carboxyl, lactone and phenol groups (Li et al. 2003) and Na_2CO_3 neutralizes carboxylic and lactonic groups (Momcilovic et al. 2011). In Table 13, the acidic functional groups corresponding to the specific neutralizing chemical are shown.

The structure of basic groups has long been a matter of dispute. It has been claimed that the structure of these groups cannot be explained as a well-defined oxygen structure. Moreover, it has been stated that the basic character of carbon cannot be attributed to the presence of chromene or any other oxygen surface functional groups (Puri 1970). Since the basicity is not entirely linked to surface oxygen complexes, it is difficult to thoroughly comprehend the nature of surface basicity of carbon (Marsh and Rodriguez Reinoso 2006).

Fourier transform infrared spectroscopy

Infrared spectroscopy is a traditional and convenient method in classifying the surface functional groups. It is based on the fact that certain infrared radiations are absorbed by specific bonds within a compound (Marsh and Rodriguez Reinoso 2006). The FTIR spectrum of the charred carbon is shown in Fig. 16.

The region from 4,000 to 1,300 cm^{-1} is specifically useful for detecting the presence of certain functional groups. The FTIR spectra reveals a broad and intense band at around 3,500 cm^{-1} which can be attributed to O–H stretching of carboxylic and phenolic groups (Mahalakshmy et al. 2009). These groups were already detected by Boehm titration.

The band present at 3,034 cm^{-1} can be attributed to C–H stretching of aromatic rings. It is mentionable the position of this band is to the left of 3,000 cm^{-1}. In case of C–H stretches which are placed to the right of 3,000 cm^{-1}, this band is attributed to alkyl C–H stretches. The spectra of simple alkanes are characterized by absorptions due to C–H stretching and bending (the C–C stretching and bending bands are either too weak or of too low a frequency to be detected in IR spectroscopy). Thus, the low-intensity band at 2,893 cm^{-1} may be linked to C–H stretches. Nevertheless, as many organic compounds have these properties, these C–H vibrations are often not mentioned when interpreting a typical IR spectrum. This is a very useful tool for

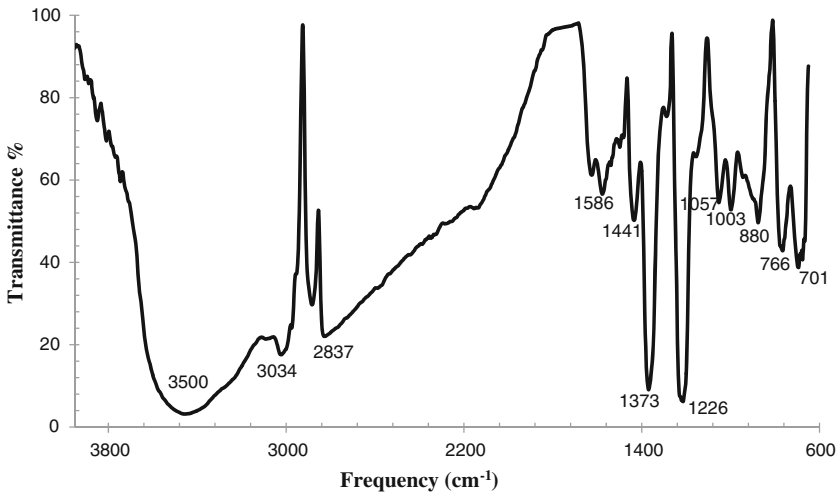

Fig. 16 FTIR spectrum of charred carbon

interpreting IR spectra: Only alkenes and aromatics show a C–H stretch slightly higher than 3,000 cm^{-1}. Compounds that do not have a C=C bond show C–H stretches only below 3,000 cm^{-1} (University of Colorado 2011).

Carboxylic acids show a strong, wide band for the O–H stretch. Unlike the O–H stretch band observed in alcohols, the carboxylic acid O–H stretch appears as a very broad band in the region 3,300–2,500 cm^{-1}. Thus, a carboxylic acid shows a somewhat "messy" absorption pattern in the region 3,300–2,500 cm^{-1}. Therefore, the stretching at 2,837 cm^{-1} can be an indication of the presence of O–H stretching in carboxylic functional groups (University of Colorado 2011).

The low intensity and weak peak at 1,586 cm^{-1} can be linked to C–C stretches in aromatic rings. C–C stretch (in-ring) shows bands in the region from 1,600 to 1,585 cm^{-1}. It is mentionable that this band has been observed by many researchers and has been interpreted unequivocally. It may be also attributed to hydrogen bonded C=O (Moreno-Castilla et al. 1998).

Another weak band was detected at 1,441 cm^{-1} which is similarly associated with C–C stretches in aromatic rings. C–C stretch (in-ring) also shows bands in the region from 1,500 to 1,400 cm^{-1}. This band may also be linked to carboxyl groups or carboxyl-carbonates structures (Moreno-Castilla et al. 1998).

Another band was detected at 1,373 cm^{-1} which can be attributed to the bending vibrations of CH_3 deformation. These deformations are found between the frequencies of 1,370–1,390 having a medium intensity (Michigan State University 2013).

Another band was detected at 1,226 cm^{-1}. This may be attributed to C–O stretches in carboxyl groups. In addition, lactones may also produce peaks in the region of 1,160–1,370 cm^{-1} (Fanning and Vannice 1993).

The bands in the region of 1,000 to 1,200 cm^{-1} are difficult to specifically qualify due to the superposition of a number of broad overlapping bands (Moreno-Castilla et al. 1998).

The region between 600 and 1,000 cm^{-1} is known as the fingerprint region. The band at 701 cm^{-1} stretch is attributed to CBr.

Conclusions

Used cigarette filters, made up of mostly cellulose acetate fibers, have proven to be potentially suitable carbon precursors for the production of porous charred carbon. Not only is it a decent way to recycle these environmentally unfriendly wastes but it can also lead to the production of more economical porous carbon when the production of activated carbon is currently costly. Moreover, the proximate analysis of used cigarette filters showed little amount of ash (0.096 %) present in the carbon precursor which is an advantage to the selection of the raw material.

The pyrolysis conditions, i.e., carbonization temperature, heating rate and soaking time were observed to be critical parameters affecting the final carbon physical properties. The effects of these parameters on the BET surface area of the final charred carbon were studied by applying a full factorial design of experiments with three factors in three levels of values, resulting in 27 runs. Amongst the pyrolysis parameters, carbonization temperature had the most significant effect on the BET porous surface area of the final product according to the statistical analyses of the results using ANOVA approach. Based on the ANOVA output, a range of linear and non-linear response surface models (RSM) were put into practice. The modeling outputs suggested that the quadratic RSM model with a reasonably appropriate R^2 value of 63 % was the best model to be developed. The optimum conditions for the production of charred carbon with maximum BET

surface area under the studied conditions were observed to be at a carbonization temperature of 900 °C, a heating rate of 5 °C/min and a soaking time of 3 h. Under these optimum conditions, the synthetic carbon showed a maximum BET surface area of 597 m^2/g.

The surface characterization of the synthesized carbon showed a complete deformation of the original raw matter from that of the final charred carbon in terms of surface morphology. The charred carbon had a surface with macro pores facilitating the bulk mass transfer into the smaller pores and thus accelerating the rate of the adsorption processes. The produced carbon also benefitted from a certain degree of mesoporosity (type IV nitrogen adsorption isotherm) with an average pore width of 3.32 nm. This implies that the synthesized carbon can be also used in the adsorption of larger molecules such as dyes. Also the adsorption of smaller molecules and chemical species can be facilitated owing to the presence of larger mesopores resulting in a faster mass transfer.

The EDX showed a certain amount of ash, e.g., Al, K and Ti still present in the final carbon even after a complete washing up of the synthesized carbon. This is an issue to be considered when the application targets the treatment of water for human consumption since even the trace amount of these metals may cause severe problems when consumed by humans. Alternative washing methods, i.e., applying diluted acids can also be later studied to assess their capability to remove these trace heavy metals in the carbon for sensitive applications.

In terms of chemical properties of the carbon surface, Boehm titration confirmed the dominant presence of acidic surface functional groups on carbon surface with a value of 0.7671 mmol/g. The degree of basicity of the carbon surface (0.0116 mmol/g) was negligible compared to its acidity. This implies that the carbonized product can be more favored to be used in the adsorption of charged species such as heavy metals. The nature of surface functional groups was believed to be more that of phenolic and carboxyl types. FTIR spectrums and bands were also applied to further confirm the presence of such functional groups on the surface of active carbon with the results being consistent with that of Boehm titration.

The cost of the production of adsorbent is often the most critical parameter which needs to be taken into account (Grini et al. 2007). Bailey et al. (1999) highlighted the fact that a sorbent is said to be low cost if it requires little processing, is abundant in nature or is the by-product or waste of another industry. Cigarette filters are one of the largest solid wastes in the world and are readily found almost everywhere. They are also a rich source of carbon due to the constructing material, i.e., cellulose acetate. However, there seems to be challenges yet to tackle. These mainly include the followings:

1. There is no adapted available strategy to collect the thrown-away cigarette butts for the purpose of recycling.
2. The current carbon yield (approximately 15 %) still needs to be improved to make the process more economical.
3. The surface area of the final carbon can be further increased by applying various activation techniques.

A further study can potentially target the activation of the produced charred carbon by applying various activation methods, i.e., chemical or physical. This will possibly improve the degree of porosity in the carbon. The activation parameters can be further adjusted and studied to tailor-make the porosity for a particular application such as catalysis, specific adsorptions and, etc. This can be done to produce an activated carbon with a more uniform PSD. In addition, the activation can be applied to enhance the degree of mesoporosity in this carbon which can alternatively suit several specific applications such as the adsorption of chemicals of specific sizes. This may even result in the production of ordered mesoporous carbons.

Another research may aim to identify a suitable set of solvent and pore-forming agents such as surfactants which can potentially create ordered mesopores under appropriate synthetic conditions. To do so, either soft-template or hard-template methods may be investigated. However, the challenge seems to be the identification of a suitable solvent which can dissolve both cellulose acetate fibers of cigarette filters and the pore-forming agent simultaneously and effectively.

A further study can be focused on improving the washing-up stage of the carbon to remove the trace amounts of heavy metals. This will enable the produced carbon to broaden its applications in the production of drinking water and/or more sensitive industrial fields.

Acknowledgments The authors would like to appreciate the University of Nottingham, Malaysia Campus, for providing us the required facilities and support to conduct this study.

References

Acikalin K, Karaca F, Bolat E (2012) Pyrolysis of pistachio shell: effects of pyrolysis conditions and pyrolysis of products. Fuel 95:169–177

Alkhatib MF, Muyibi SA, Amode JO (2011) Optimization of activated carbon production from empty fruit bunch fibers in one-step steam pyrolysis for cadmium removal from aqueous solution. Environmentalist 31:349–357

ASTM International (1996–2012). Retrieved 10 Oct 2012, from http://www.astm.org/Standard/index.shtml

Bailey SE, Olin TJ, Bricka R, Adrian D (1999) A review of potentially low-cost sorbents for heavy metals. Water Res 33(11):2469–2479
Bansal RC, Goyal M (2005) Activated carbon adsorption. Tayler & Francis Group, Boca Raton
Barbooti MM, Mohammad TJ, Hussain AA, Abas FO (2004) Optimization of pyrolysis conditions of scrap tires under inert gas atmosphere. J Anal Appl Pyrol 72:165–170
Barnes R (2011) Regulating the disposal of cigarette butts as toxic hazardous waste. Tobacco control 20:i45–i48
Bhole V, Ramteke DS (2011) Preferential adsorption of heavy metals on activated carbon. Bangladesh J Sci Ind Res 46(2):211–218
Bouchelta C, Medjram MS, Zoubida M, Chekkat FA, Ramdane N, Bellat JP (2012) Effects of pyrolysis conditions on the porous structure development of date pits activated carbon. J Anal Appl Pyrolysis 94:215–222
Dias JM, Alvim-Ferraz MC, Almeida MF, Rivera-Utrilla J, Sanchez-Polo M (2007) Waste materials for activated carbon preparation and its use in aqueous-phase treatment: a review. J Environ Manag 85:833–846
Fanning P, Vannice M (1993) A DRIFTS study of the formation of surface groups on carbon by oxidation. Carbon 31(5):721–730
Fowles J, Bates M (2000) The chemical constituents in cigarettes and cigarette smoke: priorities for harm reduction. New Zealand Ministry of Health
Fu P, Hu S, Xiang J, Sun L, Su S, Wang J (2012) Evaluation of the porous structure development of chars from pyrolysis of rice straw: effects of pyrolysis temperature and heating rate. J Anal Appl Pyrolysis 98:177–183
Gregg S, Sing K S (1982) Adsorption, surface area and porosity. London, Academic Press
Ginot V, Gaba S, Beaudouin R, Aries F, Monod H (2006) Combined use of local and ANOVA-based global sensitivity analyses for the investigation of a stochastic dynamic model: application to the case study of an individual-based model of a fish population. Ecol Model 193:479–491
Grini G, Peindy HN, Gimbert F, Robert C (2007) Removal of C.I. basic green 4 from aqueous solutions by adsorption using cyclodextrin-based adsorbent: kinetic and equilibrium studies. Sep Purif Technol 53:97–110
Haykiri-Acma H, Yaman S, Kucukbayrak S (2006) Effect of heating rate on the pyrolysis yields of rapeseed. Renew Energy 31:803–810
Jia Q, Lua AC (2008) Effects of pyrolysis conditions on the physical characteristics of oil-palm-shell activated carbons used in aqueous phase phenol adsorption. J Anal Appl Pyrolysis 83:175–179
Lafi WK (2001) Production of activated carbon from acorns and olive seeds. Biomass Bioenergy 20:57–62
Laszlo K, Bota A, Nagy LG (2000) Comparative adsorption study on carbons from polymer precursors. Carbon 38:1965–1976
Li YH, Lee CW, Gullett BK (2003) Importance of activated carbon/s oxygen surface functional groups on elemental mercury adsorption. Fuel 82:451–457
Li L, Liu S, Liu J (2011) Surface modification of coconut shell based activated carbon for the improvement of hydrophobic VOC removal. J Hazard Mater 192:683–690
Longwood Education (2011). Retrieved 12 Dec 2011, from http://www.longwood.edu/cleanva/cigbuttfilters.htm
Lua AC, Yang T, Guo J (2004) Effect of pyrolysis conditions on the properties of activated carbons prepared from pistachio-nut shells. J Anal Appl Pyrolysis 72:279–287
Lua AC, Lau FY, Guo J (2006) Influence of pyrolysis conditions on pore development of oil-palm-shell activated carbons. J Anal Appl Pyrol 76:96–102
Mahalakshmy R, Indraneel P, Viswanathan B (2009) Surface functionalities of nitric acid treated carbon—a density functional theory based vibrational analysis. Indian J Chem 18A:352–356
Malekbala M, Hosseini S, Yazdi SK, Masoudi Soltani S, Malekbala M (2012) The study of the potential capability of sugar beet pulp on the removal efficiency of two cationic dyes. Chem Eng Res Des 90:704–712
Marsh H, Rodriguez Reinoso F (2006) Activated carbon, 1st edn. Elsevier, Oxford
Michigan State University (2013) Infrared Spectroscopy. Retrieved 22 Feb 2013, from http://www2.chemistry.msu.edu/faculty/reusch/VirtTxtJml/Spectrpy/InfraRed/infrared.htm
Moerman J, Potts G (2011) Analysis of metals leached from smoked cigarette litter. Tobacco Control 20:i30–i35
Momcilovic M, Purenovic M, Bojic A, Zarubica A, Randelovic M (2011) Removal of lead (II) ions from aqueous solutions by adsorption onto pine cone activated carbon. Desalination 276:53–59
Montgomery DC, Runger GC (2011) Applied statistics and probability for engineers, 5th edn. John Wiley and Sons, Inc, Asia
Moreno-Castilla C, Carrasco-Marin F, Maldonado-Hodar FJ, Rivera-Utrilla J (1998) Effects of non-oxidant and oxidant acid treatments on the surface properties of an activated carbon with very low ash content. Carbon 36:145–151
Nogi K, Naito M, Yokoyama T (2012) Nanoparticle technology handbook, 2nd edn. Elsevier, Amsterdam
Novotny ET, Lum K, Smith E, Wang V, Barnes R (2009) Filtered cigarettes and the case for an environmental policy on cigarette waste. Int J Environ Res Public Health 6. doi:10.3390/ijerph60x000x
Novotny ET, Hardin SN, Hovda LR, Novotny DJ, McLean MK, Shan S (2011) Tobacco and cigarette butt consumption in humans and animals. Tobacco J 20(1):i17–i20
Ojeda M, Esparza JM, Campero A, Cordero S, Kornhauser I, Rojas F (2003) On comparing BJH and NLDFT pore-size distributions determined from N2 sorption on SBA-15 substrata. Phys Chem Chem Phys 5:1859–1866
Polarz S, Smarsly B, Schattka JH (2002) Hierarchical porous carbon structures from cellulose acetate fibers. Chem Mater 14(7):2940–2945
PubChem Compound (2011) (National Center for Biotechnology Information, U.S. National Library of Medicine), Retrieved 15 Jan 2013, from http://pubchem.ncbi.nlm.nih.gov/summary/summary.cgi
Puri BR (1970). In: Walker PL Jr (ed) Chemistry and physics of carbon, vol 6. Marcel Dekker, New York, p 191
Rodrigues Filho G, Monteiro DS, Cd Meireles, de Assuncao RM, Cerqueira DA, Barud HS, Messadeq Y (2008) Synthesis and characterization of cellulose acetate produced from recycled newspaper. Carbohydr Polym 73:74–82
Rodriguez-Reinoso F, Sepulveda-Escribano A (2001) Porous carbons in adsorption and catalysis. In: Handbook of surfaces and interfaces of materials, vol 5. Academic Press, London
Smith EA, Novotny TE (2011) Whose butt is it? Tobacco industry research about smokers and cigarette butt waste. Tobacco J 20:i2–i9
Stavropoulos GG, Samaras P, Sakellaropoulos GP (2008) Effect of activated carbons modification on porosity, surface structure and phenol adsorption. J Hazard Mater 151:414–421
Sudaryanto Y, Hartono SB, Irawaty W, Hindarso H, Ismadji S (2006) High surface area activated carbon prepared from cassava peel by chemical activation. Bioresour Technol 97:734–739
Tao X, Xiaoqin L (2008) Peanut shell activated carbon: characterization, surface modification and adsorption of Pb2+ from aqueous solution. Chin J Chem Eng 16(3):401–406
University of Colorado BC (2011) IR spectroscopy tutorial. Retrieved 22 Feb 2013, from http://orgchem.colorado.edu/Spectroscopy/irtutor/tutorial.html
Yin CY, Aroua MK, Wan Daud WM (2007) Review of modifications of activated carbon for enhancing contaminant uptakes from aqueous solutions. Sep Purif Technol 52:403–415